PHASE DIAGRAMS, STRUCTURAL AND THERMODYNAMIC PROPERTIES OF MOLTEN SALT SOLVENTS FOR THE INDUSTRIAL SO_2-OXIDATION CATALYST

Rasmus Fehrmann
Technical University of Denmark

Soghomon Boghosian
University of Patras / Institute of Chemical Engineering
and High Temperature Chemical Processe, Greece

Hind Hamma-Cugny & Jacques Rogez
Université Paul Cézanne, France

ABSTRACT

The molten salt system $Rb_2S_2O_7$ - $RbHSO_4$ and its analogous Na, K and Cs systems have been the subject of our systematic investigations regarding their physical and chemical properties as well as properties as solvents for vanadium oxides leading to formation of vanadium complexes, active as catalysts for oxidation of SO_2 in sulfuric acid production. The present work reports the electrical conductivities of 14 different compositions of the binary $Rb_2S_2O_7$ - $RbHSO_4$ system in the temperature range 430-470 K. Based on these measurements and thermal measurements of selected compositions of the binary system, the heat of mixing and the phase diagram of the $Rb_2S_2O_7$ - $RbHSO_4$ system could be constructed. The melting temperatures of the pure components, $Rb_2S_2O_7$ and $RbHSO_4$, were found to be 718 K and 487 K, respectively while the phase diagram was found to be of the simple eutectic type with an eutectic composition of mole fraction $X(RbHSO_4)=0.92$ and melting temperature of 471 K. These values are compared to those found previously for the Na, K and Cs analogue, exhibiting a systematic trend for these binary alkali metal salt systems.

INTRODUCTION

The molten salt – gas system $M_2S_2O_7$-M_2SO_4-V_2O_5/SO_3-SO_2-O_2-N_2 (M=alkali) at 400-500°C is a realistic model for the working molten vanadium – based SLP (supported liquid phase) catalysts used for the oxidation of SO_2 to SO_3 [1]. The same catalysts are used for the desulphurization of wet industrial flue gases, where SO_2 is oxidized to SO_3 and subsequently condensed as H_2SO_4 [2]. The presence of water vapor either in the flue gas or in the feed gas of the *wet* sulfuric acid process results in a partial transformation of the alkali pyrosulfates (e.g. $K_2S_2O_7$) to the corresponding hydrogen sulfates ($KHSO_4$) in accordance with the equilibrium

$$2HSO_4^-(l) \leftrightarrow S_2O_7^{2}(1) + H_2O(g) \quad (1)$$

Thus, physicochemical information about the molten $M_2S_2O_7$ - $MHSO_4$ solvent systems is highly important for the understanding of the working catalyst in the wet SO_2 oxidation processes. Therefore, the $M_2S_2O_7$ - $MHSO_4$ (M=Na, K, Rb and Cs) systems have been investigated by calorimetry, conductivity, NMR, NIR and Raman spectroscopy and phase diagrams of the corresponding binary systems have been constructed [3, 4, 5]. All systems are of the simple eutectic form with no intermediate compound formation. The spectroscopic investigations show [6] that the dominant species in the melt are $S_2O_7^{2-}$ and HSO_4^- ions with traces of H_2O probably being present. The water molecules could probably be associated to the other constituents of the melts by hydrogen bonding, even at 450°C (typical catalyst operation temperature). The results might be useful for the design of SO_2 oxidation catalysts being able to operate below 350°C, making single absorption of SO_3 possible instead of the double absorption process used in modern sulfuric acid plants. Here we will focus on the results so far for the $Rb_2S_2O_7$-$RbHSO_4$ system and compare to the other similar alkali systems studied previously by us.

EXPERIMENTAL

Chemicals

Pure $M_2S_2O_7$ salts are either not commercially available (Rb, Cs) or seriously contaminated by hydrogen sulfates (Na, K) due to their hygroscopicity. Therefore, pure and dry commercial $M_2S_2O_8$ (Merck, p.a.) in the case of Na and K was used, while the non-commercially available peroxo-disulfates $Rb_2S_2O_8$ and $Cs_2S_2O_8$ were synthesized in the laboratory as earlier described [7, 8]. The commercial available NaHSO4 and KHSO4 (Merck, suprapur (99%)) were dried at 110°C while the non-commercial available RbHSO4 and $CsHSO_4$ were synthesized by adding carefully weighed amounts of water to the respective pyrosulfates in ampoules. The ampoules were then sealed and equilibrated by slow stepwise heating to 230 - 250°C. The purity was checked by Raman spectroscopy [9] on the molten salt showing less than 0,5% residual pyrosulfater. All handlings of the hygroscopic alkali pyrosulfates and hydrogen sulfates were performed in a glovebox with a water content of less than around 5 ppm. All chemicals were kept on ampoules, only opened in the glovebox, and resealed immediately after use. The non-hygroscopic V_2O_5 (Cerac, pure (99,9%)) and alkali sulfates M_2SO_4 (Merck, p.a.) could be kept outside the glovebox and used without further treatment. Commercial N_2 and Ar were used and, when necessary, dried through P_2O_5 columns.

Conductivity

The conductivity cell is made of borosilicate glass, where gold electrodes are fused into the bottom of the two compartments containing the melt, in contact via a capillary tube of around 1mm i,d., as described earlier in detail [10]. The cell was loaded by cutting the stem open in the glovebox. The furnace was regulated within ±0.1°C, and the temperature of the melt was decreased in steps of 5-10°C until the subcooled melt suddenly crystallized, indicated by large drop of the electrical conductivity. The temperature was then increased in steps of 0.5-2°C close to the phase transitions and 5-10°C far from these transitions until the initial temperature of the melt was reached and the reproducibility of the conductivity checked. The conductivity was measured by a radiometer CDM-230 conductivity meter, the temperature obtained by chromel-alumel thermocouples calibrated against a Pt100 resistance thermometer, and the cell constants of the order of 100-200 cm^{-1} were found using 0.1 D KCl standard solution as previously described [11].

Isothermal Calorimetry

The melting temperatures of pure $Rb_2S_2O_7$ and $RbHSO_4$ are very different and we could not measure the liquid heat of mixing of this binary system over the full concentration range. Indeed, $RbHSO_4$ decompose around 30°C above its melting point. The measurements were carried out at 505 K where $RbHSO_4$ is in the liquid state, whereas $Rb_2S_2O_7$ is always solid. By taking into account the enthalpy of fusion of $Rb_2S_2O_7$, we could reference our results to the liquid state and we could obtain the excess enthalpies of mixing $Rb_2S_2O_7$ in $RbHSO_4$ both in the liquid state at different concentrations. The partial enthalpies of mixing of $Rb_2S_2O_7$ in $RbHSO_4$ in the binary system were measured by using a Calvet micro calorimeter. Measurements were carried out by breaking fragile ampules with $Rb_2S_2O_7$ in the $Rb_2S_2O_7$-$RbHSO_4$ melt containing crucibles (after the ampules had been thermally equilibrated). The calibration of the calorimeter was performed after each experiment by dropping pure gold (5N) samples in the same experimental cell.

Phase Diagram Determined by DSC

To verify the transition temperatures obtained by electrical conductivity, four different samples have been investigated by differential scanning calorimetry. Alkali pyrosulfates and hydrogensulfates could be considered as simple salts for which, when heated, the most common reactions occurring are melting, dissociation, dehydration, decomposition, polymorphic transition and hydrolysis. Other processes such as transition from metastable to stable states, crystal growth, oxidation, etc. can also occur. The interpretation of the thermal effects was delicate since the samples with admixtures exhibit several overlapping peaks that we couldn't associate to any melting phenomena or appearance of new phases but possibly could be referred to polymorphic transitions. Pure $Rb_2S_2O_7$ melts at 723 K with an associated heat of fusion H_{fus} = 17849 $J{\cdot}mol^{-1}$. These values are in excellent agreement with the previously [12] published values of 723 K and 18000 $J{\cdot}mol^{-1}$, respectively. The premelting effect detected 50 K below the melting point explains the small discrepancies between the different experimental methods used for the phase transition determination. $RbHSO_4$ thermograms exhibit an onset temperature at 480 K, this value is different from the one deduced from conductivity measurements i.e., 487 K. However, the top of the DSC peak is at 487 K. A heat flux DSC 111 (Setaram) was used. It is equipped with two cylindrical cavities - each could contain the sample or the reference- connected to a furnace by multiple thermocouples which constitute a good heat flux measure. The ampules were filled in the glove box and sealed. The accuracy of the measurements was ±2 K in the temperature range investigated.

RESULTS AND DISCUSSION

Conductivity Measurements

The conductivity of the $Rb_2S_2O_7$-$RbHSO_4$ binary system has been measured at 14 different concentrations in the temperature range 430-740 K. The results are shown in Figure 1.

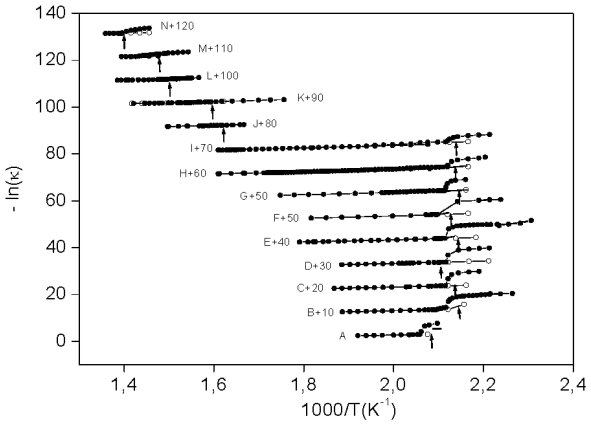

Figure 1: Electrical conductivity, κ, vs 1/T for the $Rb_2S_2O_7$-$RbHSO_4$ system at various compositions X($RbHSO_4$): A,1.00; B,0.9048; C, 0.8690; D,0.8390; E,0.8064; F, 0.7447; G 0.7045, H 0.6005; I,0.4996; J, 0.3983; K,0.2995; L,0.2038; M,0.0956 ; N,0.00. Open circles indicate subcooling and arrows indicate liquidus temperatures.

The samples rich in $RbHSO_4$ crystallize rather easily and large jumps of the conductivity to lower values are observed by crystallization. By reheating in small steps, i.e., 1-2°C, the fusion of the eutectics (the solidus temperature) could be observed as breaks at 471 K and an accurate value of the liquidus temperature was obtained for the following concentrations X($RbHSO_4$) =0.4996; 0.6005; 0.7045; 0.7447; 0.8064; 0.8390 and 0.9048. For the $Rb_2S_2O_7$ rich mixtures: X($RbHSO_4$) = 0.3983; 0.2995; 0.2038; 0.0956. It was difficult to state the phase changes. On account of the (-lnκ,1/T) plots, we display in Table 1 the different transition temperatures and the phase diagram of the $Rb_2S_2O_7$ -$RbHSO_4$ system could be outlined.

Table 1: Liquidus and solidus temperatures for the $Rb_2S_2O_7$-$RbHSO_4$ system

	X	Tliquidus	Tsolidus
	(RbHSO4)	(K)	(K)
	0	718	
	0,0956	701	
	0,2038	676	
	0,2995	653	
	0,3983	627	
	0,4996	612	472
	0,6005	582	471
	0,7045	553	472
0,7447		544	471
0,8690		486	471
0,9048		479	
1		487	

Phase Diagram

The phase diagram of the binary system $Rb_2S_2O_7$-$RbHSO_4$ is displayed in Figure 2.

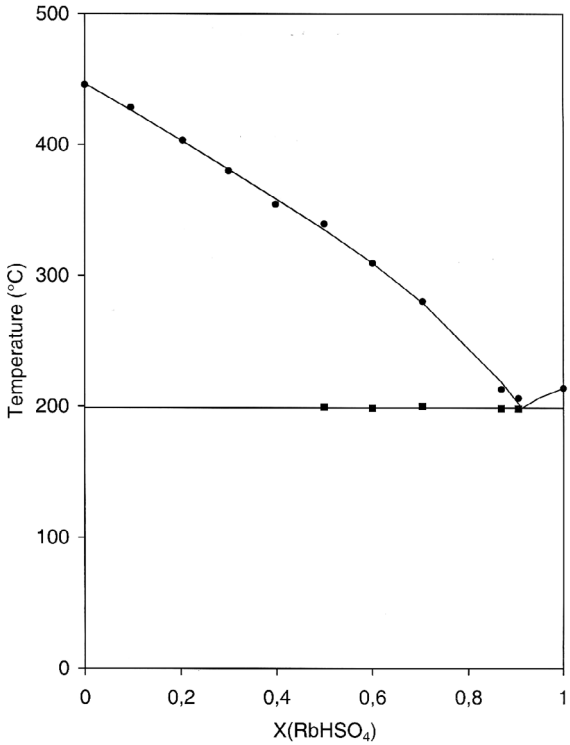

Figure 2: Phase diagram of the $Rb_2S_2O_7$-$RbHSO_4$ system based on the conductivity measurements

The points on the liquidus curve in the phase diagram have been determined by the temperatures of complete melting for all of the 14 different compositions measured by electrical conductivity measurements. The solidus and the liquidus temperatures obtained for all measurements are given in Table 1. The melting point of pure $Rb_2S_2O_7$ was found to be 723 K. For pure $RbHSO_4$, the melting point was measured to be 487 K. Because no peritectic compounds are found, the solidus line is probably representative for the whole composition range as also was the case of the Na, K and Cs equivalents of the present binary Rb system but was not investigated here at low mole fractions due to the risk of breaking the cell by cooling far below the liquidus temperatures.

CONCLUSIONS

The results presented here for the binary $Rb_2S_2O_7$-$RbHSO_4$ system are with regard to the characteristics for the eutectic composition and the partial heat of mixing given in Table 2:

Table 2: Thermal properties of the $M_2S_2O_7$-$MHSO_4$ system (M = Na, K, Rb and Cs). Compositions (Xeut) and temperatures of fusion (Tfus, eut) of the eutectics and experimental and calculated partial heats of mixing ($\Delta H\infty$) $M_2S_2O_7$ (1) in $MHSO_4$ (1) at the indicated temperatures (Tmix).

	Xeut[a]	**Tfus,eut (K)**	**$\Delta H\infty(M_2S_2O_7)$ ($J \cdot mol^{-1}$)**	**Tmix (K)**	
		exp.	calc.		
$Na_2S_2O_7$-$NaHSO_4$	0,97	452	-11950	-11940	544
$K_2S_2O_7$-$KHSO_4$	0,94	478	-20000	-20008	544
RbS_2O_7-$RbHSO_4$	0,92	471	-17800		503
CsS_2O_7-$CsHSO_4$	0,86	470	-12279	-12225	517
[a] Xeut = $X(MHSO_4)$					

The eutectic composition is estimated to be X ($RbHSO_4$) = 0.92 with a melting point of 471 K. For the analogous Na, K and Cs systems, the eutectic compositions were found at $X(NaHSO_4)$ = 0.97, $X(KHSO_4)$ = 0.94 and $X(CsHSO_4)$ = 0.86 respectively. Thus, increasing the size of the alkali cation decreases the mole fraction $X(MHSO_4)$ for the eutectic compositions. The results might be useful for the design of SO_2 oxidation catalysts used worldwide for sulphuric acid production aiming to achieve a catalyst able to operate below 350°C, thereby avoiding the undesired double absorption process design characteristic of modern sulphuric acid plants.

ACKNOWLEDGMENTS

The Danish Natural Science Research Council and ICAT (Interdisciplinary Research Center for Catalysis), DTU, Denmark have supported this investigation.

REFERENCES

Lapina, O. B., Bal´zhinimaev, B. S., Boghosian, S., Eriksen, K. M. & Fehrmann, R. (1999). *Progress on the Mechanistic Understanding of SO_2 Oxidations Catalysts*. Catalysis Today, Vol. 51, pp. 469-479. [1]

Masters, S. G., Chrissanthopoulos, A., Eriksen, K. M., Boghosian, S. & Fehrmann, R. (1997). Catalytic Activity & Deactivation of SO_2 Oxidation Catalysts in Simulated Power Plant Flue Gases. *Journal of Catalysis*, Vol. 166, pp. 16-24. [2]

Eriksen, K. M., Fehrmann, R., Hatem, G., Gaune-Escard, M., Lapina, O. B. & Mastikhin, V. M. (1996). Conductivity, NMR, Thermal Measurements, & Phase Diagram of the $K_2S_2O_7$-$KHSO_4$ System. *Journal of Physical Chemistry*, Vol. 100, pp. 10771-10778. [3]

Hatem, G., Gaune-Escard, M., Rasmussen, S. B. & Fehrmann, R. (1999). Conductivity, Thermal Measurements, & Phase Diagram of the $Na_2S_2O_7$-$NaHSO_4$ System. *Journal of Physical Chemistry*, Vol. 103, pp. 1027-1030. [4]

Hamma, H., Rogez, J., Ståhl, K., Berg, R.W. & Fehrmann, R. ( ). Thermal, Conductometric, X-Ray & Raman Spectroscopic Investigations & Phase Diagram of the $Rb_2S_2O_7$-$RbHSO_4$ System. *Journal of Physical Chemistry B*, to be submitted. [5]

Knudsen, C., Kalampounias, A. G., Fehrmann, R. & Boghosian, S. (2008). Thermal Dissociation of Molten $KHSO_4$: Temperature Dependence of Raman Spectra & Thermodynamics. *Journal of Physical Chemistry B*, Vol. 112, pp. 11996-12000. [6]

Boghosian, S., Fehrmann, R., Bjerrum, N. J. & Papatheodorou, G. N. (1989). Formation of Crystalline Compounds & Catalyst Deactivation during SO_2 Oxidation in V_2O_5 -$Na_2S_2O_7$, V_2O_5-$K_2S_2O_7$, V_2O_5 - $CS_2S_2O_7$, *Melts*. *Journal of Catalysis,* Vol. 119, pp. 121-134. [7]

Folkmann, G. E., Hatem, G., Fehrmann, R., Gaune-Escard, M. & Bjerrum, N. J. (1991). *Conductivity, Thermal-Analysis & Phase-Diagram of the system $CS_2S_2O_7$ -V_2O_5. Spectroscopic Characterization of $Cs_4(VO_2)_2(SO_4)2S_2O_7$*. Inorganic Chemistry Vol. 30, pp. 4057-4061. [8]

Fehrmann, R., Hansen, N. H. & Bjerrum, N, J. (1983). *Raman-Spectroscopic & Spectrophotometric Study of the system $K_2S_2O_7$ -$KHSO_4$ in the temperature-range 200-450°C*. Inorganic Chemistry Vol. 22, pp. 4009-4014. [9]

Eriksen, K. M., Fehrmann, R., Hatem, G., Gaune-Escard, M., Lapina, O. B. & Mastikhin, V. M. (1996). Conductivity, NMR, Thermal Measurements, & Phase Diagram of the $K_2S_2O_7$ - $KHSO_4$ System. *Journal of Physical Chemistry*, Vol. 100, pp. 10771-10778. [10]

Jones, G., Bradshaw, B. C. (1933). The Measurement of the Conductance of Electrolytes. V. A Redetermination of the Conductance of Standard Potassium Chloride Solutions in Absolute Units. *Journal of the American Chemical Society*, Vol. 55, pp. 1780-1800. [11]

Hatem, G. K., Eriksen, M., Gaune-Escard, M. & Fehrmann, R. (2002). *SO_2 Oxidation Catalyst Model Systems Characterized by Thermal Methods*. Topics in Catalysis, Vol. 19, pp. 323-331. [12]